Journal of Molecular Catalysis A: Chemical 355 (2012) 75–84

Contents lists available at SciVerse ScienceDirect

Journal of Molecular Catalysis A: Chemical

journal homepage: www.elsevier.com/locate/molcata

The use of bimetallic MCM-41 mesoporous catalysts for the synthesis of MWCNTs by chemical vapor deposition

R. Atchudan [a], A. Pandurangan [a,b,*]

[a] Department of Chemistry, Anna University, Chennai 600025, India
[b] Institute of Catalysis and Petroleum Technology, Anna University, Chennai 600025, India

ARTICLE INFO

Article history:
Received 18 July 2011
Received in revised form
29 November 2011
Accepted 30 November 2011
Available online 8 December 2011

Keywords:
MWCNT
CVD
Cr-MCM-41
Fe/Cr-MCM-41
Acetylene
Mesoporous catalyst

ABSTRACT

Mesoporous MCM-41 molecular sieves incorporating chromium with different Si/Cr ratios (Si/Cr: 50, 75, 100 and 125) were synthesized hydrothermally and Co, Fe, Mn, Ni, Ti, Ru, and Pd were loaded on them using wet impregnation method. The synthesized materials were characterized by various physico-chemical techniques, such as ICP-AES, XRD, TGA, N_2 sorption isotherms, DRS-UV and TEM. The production of MWCNTs by CVD using metal-containing mesoporous MCM-41 was investigated using acetylene as the carbon source. Fe/Cr-MCM-41 and Pd/Cr-MCM-41 are the most active catalysts for the growth of MWCNTs when compared with the other mono and bimetallic mesoporous catalysts. The MWCNTs have been analyzed by XRD, SEM, TGA, TEM and Raman spectroscopy. The strongest peak of the graphite band and the weak disorder band in the Raman spectrum confirmed the high purity of the MWCNTs. The structure of MWCNTs was studied by TEM which suggests that they are highly ordered and well graphitized. The formation of MWCNTs with uniform inner diameter in the range of 4–5 nm and outer diameter in the range of 12–13 nm was observed over Fe/Cr-MCM-41. These studies suggest that the bimetallic MCM-41 could be a kind of promising supports for catalytically synthesizing MWCNTs by CVD method.

1. Introduction

Carbon nanotubes (CNTs) have attracted a great deal of interest by the research community due to their unique and useful chemical and physical properties [1,2]. CNTs have shown promising prospect in a wide range of applications such as electronic devices [3], energy storage [4], drug delivery [5], etc. The syntheses have involved three main approaches [6], namely, (i) arc discharge between two graphite electrodes, (ii) laser evaporation of carbon target and (iii) chemical vapor deposition (CVD) through catalytic decomposition of hydrocarbons. The first two methods employ the solid-state carbon precursors needed for carbon evaporation at high temperature. The CVD utilizes hydrocarbon gases as carbon sources and metal nanoparticles as the seeds for the growth of CNT. Of these, the CVD is the most promising and versatile since it allows easy scale-up and directed placement, alignment of nanotubes and construction of electronic components [7]. The catalytically produced tubes are adequate for many applications, especially in electronic devices because they can be directly synthesized without major contamination by carbonaceous impurities.

In 1992, researchers at Mobil Research and Development Corporation reported the synthesis of a new family of mesoporous molecular sieves (M41S) with exceptionally large uniform pore structures [8,9]. Transition metal can be incorporated into the pore walls of the mesoporous molecular sieves stabilizing dispersed catalytic sites and also exhibit good structural stability. The M41S family containing MCM-41 and related mesoporous molecular sieves are of interest because of their remarkable properties, such as large surface area (>1000 m^2/g), pore volume (>0.8 cm^3/g), narrow pore size distribution and the ease with which their surface can be functionalized [9]. Also, their uniform and tunable pore diameters make them well adapted as good catalytic supports. Generally, pure siliceous MCM-41 has limited catalytic activity, but active catalytic sites can be generated in Si-MCM-41 by isomorphously substituting silicon with transition metal [10]. Several studies have been dedicated to the investigation of transition metal substituted MCM-41 because of their wide range of applications in catalysis [11,12]. Apart from catalysis, the metal-containing MCM-41 also used a catalytic template for the synthesis of CNTs. The metal particle plays an important role during CNT production and reports abound, showing a direct correlation between the size of the metal nanoparticles and the eventual tube diameter [13].

* Corresponding author at: Department of Chemistry, Anna University, Chennai 600025, India. Tel.: +91 44 22358653; fax: +91 44 22200660.
E-mail address: pandurangan_a@yahoo.com (A. Pandurangan).

1381-1169/$ – see front matter © 2011 Elsevier B.V. All rights reserved.
doi:10.1016/j.molcata.2011.11.028

During catalytic chemical vapor deposition, CNTs grow by the catalytic decomposition of acetylene gas over the metal particles embedded in mesoporous MCM-41 supports. Transition metals have been widely used either in oxide or in metallic forms or as mixtures, as they possess a variety of properties that render them suitable for CNT synthesis such as equilibrium vapor pressure, solubility of carbon and carbon diffusion rate in the metal [14]. Many parameters including temperature and duration of the CVD, gas composition and flow rate can affect the nature of the carbon deposits in the resulting material [15]. The number of studies show the role of transition metal incorporated mesoporous MCM-41 material for the synthesis of CNTs, but there is a limitation in the systematic study of bimetal-containing mesoporous materials for improving the yield and quality of CNT. In the present study, the chromium incorporated mesoporous MCM-41 molecular sieves with different Si/Cr ratios (Si/Cr: 50, 75, 100 and 125) were synthesized hydrothermally and Co, Fe, Mn, Ni, Ti, Ru and Pd were loaded on them using wet impregnation method. The above-prepared materials act as catalytic templates and acetylene was used as carbon precursor for the growth of multi-walled carbon nanotubes (MWCNTs) by CVD with high quality and large quantity. The effect of reaction parameters such as temperature and bimetals for the growth of CNTs were studied. The synthesized materials were investigated by various physico-chemical techniques such as Inductive Coupled Plasma-Atomic Emission Spectroscopy (ICP-AES), X-ray diffraction (XRD), N_2 sorption isotherms, thermogravimetric analysis (TGA), diffuse reflectance ultra violet-visible spectroscopy (DRS-UV), scanning electron microscopy (SEM), transmission electron microscopy (TEM) and Raman spectroscopy.

2. Experimental

2.1. Materials

The chemicals used for the synthesis of metal-containing mesoporous molecular sieves were sodium metasilicate (Qualigens), cobalt nitrate (Merck), ferric nitrate (Merck), manganese acetate (Merck), nickel nitrate (Merck), titanium chloride (Merck), ruthenium chloride (Merck) and palladium chloride (Merck) as a source of Si, Co, Fe, Mn, Ni, Ti, Ru and Pd, respectively. Cetyltrimethylammonium bromide (CTAB) (Merck) was used as the structure-directing agent. Sulphuric acid (Merck) was used to adjust the pH of the medium. Hydrofluoric acid (Merck), hydrochloric acid (Merck) and nitric acid (Merck) were used for the purification of CNTs.

2.2. Synthesis of Cr-MCM-41 molecular sieves

Cr-MCM-41 molecular sieves with different Si/Cr ratios of 50, 75, 100 and 125 were synthesized hydrothermally using the gel composition of SiO_2:xCr_2O_3:0.2CTAB:0.89H_2SO_4:120H_2O. In a typical synthesis, 28.42 g of sodium metasilicate was dissolved in distilled water and required amount of chromium nitrate solution was added after 30 min of stirring. The pH of the solution was adjusted to 10.5 with constant stirring to form a gel. After 30 min, an aqueous solution of CTAB was added and then the mixture was stirred for 1 h at room temperature. The suspension was then transferred into a 300 mL stainless steel autoclave, sealed and heated in hot air oven at 150 °C for 48 h. After cooling to room temperature, the formation of the product was filtered and then washed with distilled water and dried at 100 °C for 6 h. The dried material was calcined at 550 °C in atmospheric air for 5 h in a muffle furnace to expel the template.

2.3. Preparation of metal impregnated Cr-MCM-41 molecular sieves

Transition metals such as Fe, Co, Mn, Ni, Ti, Ru and Pd of 0.2 wt.% was loaded individually over Cr-MCM-41 (100) molecular sieves by wet impregnation method. In a typical procedure, the appropriate amount of iron nitrate was dissolved in distilled water and sonicated for 15 min; the sonicated solution was added drop by drop to the calcined Cr-MCM-41 (100) under constant stirring. The solution was dried under reduced pressure and calcined in atmospheric air at 550 °C for 4 h. Similar procedure was adopted for Co, Mn, Ni, Ti, Ru and Pd to obtain respective metal loaded Cr-MCM-41 (100).

2.4. Synthesis of MWCNTs

The catalytic reactions for the synthesis of MWCNTs were carried out using the various Si/Cr ratios of MCM-41 and the optimized Si/Cr ratio was taken further to study the effect of various metals such as Co, Fe, Mn, Ni, Ti, Ru and Pd by CVD. This CVD setup consists of a horizontal tubular furnace and gas flow control units. In a typical growth experiment, 200 mg of catalyst was placed in a quartz boat inside the quartz tube. The catalyst was purged in a nitrogen gas at a flow rate of 100 mL/min for 30 min to remove the water and thus to pre-treat the catalyst and then hydrogen gas at a flow rate of 100 mL/min was purged for 30 min to reduce the metal particles. The reaction was carried out using acetylene as carbon source at 800 °C with a flow rate of 100 mL/min for 30 min. The furnace was then cooled to room temperature under nitrogen atmosphere; the appearance of black material confirms the completion of the reaction. The obtained material was weighed, purified and then characterized. The percentage of the carbon deposited due to the catalytic decomposition of acetylene was calculated from the following equation:

$$\text{Carbon deposition yield}\,(\%) = \frac{m_{\text{tot}} - m_{\text{cat}}}{m_{\text{cat}}} \times 100$$

where m_{tot} is the total mass of carbon product with catalyst and m_{cat} is the mass of catalyst.

2.5. Purification of MWCNTs

The technique for the removal of the silica phase by the presence of 40% of hydrofluoric acid (HF) at ambient temperature was found in the literature [16,17]. The as-synthesized carbon sample was calcined at 450 °C in air atmosphere for 2 h in muffle furnace to remove the amorphous carbon and other carbonaceous impurities. The calcined carbon sample was immersed in an appropriate amount of HF, washed with distilled water and dried. The obtained sample was further treated with nitric acid and hydrochloric acid to remove the metal particles and then washed with distilled water and dried at 100 °C for 5 h in air atmosphere. In order to remove the carbonaceous impurities, the obtained material was subjected to air oxidation at 450 °C for 2 h in muffle furnace [18,19]. The oxidized material was cooled to the room temperature slowly and then characterized by various physico-chemical techniques.

2.6. Characterization methods

The synthesized Cr-incorporated mesoporous MCM-41, metal-impregnated Cr-MCM-41 materials and CNTs were characterized by various physico-chemical techniques such as ICP-AES, XRD, N_2 sorption isotherms, TGA, DRS-UV, SEM, TEM and Raman spectroscopy. The amount of Cr loaded in the MCM-41 molecular sieves were analyzed and determined by ICP-AES, PerkinElmer OPTIMA 3000. The samples were dissolved in a mixture of HF and HNO_3 before the measurement. The X-ray powder diffractograms of

calcined catalysts and purified MWCNT samples were recorded on a PANalytical X'Pert diffractometer equipped with liquid nitrogen cooled germanium solid-state detector using Cu Kα radiation. The diffractogram of metal incorporated MCM-41 and CNTs was recorded in the 2θ range of 1–10° and 5–80°, respectively, at the scanning rate of 0.02° with the counting time of 5 s at each point. N_2 sorption isotherms were measured at −197 °C using a Micromeritics ASAP 2000. Prior to the experiments, the samples were dried at 130 °C and evacuated overnight for 8 h in flowing argon at a flow rate of 60 mL/min at 200 °C. The surface area, pore size and pore volumes were calculated from these isotherms using the conventional Stephen Brunauer–Paul Hugh Emmett–Edward Teller (BET) and Barret–Joyner–Halenda equations. TGA of the materials were performed using a Mettler TA 3001 analyser. Samples of approximately 10 mg were heated in air from 30 to 800 °C at a heating rate of 10 °C/min. DRS-UV analysis was performed using a Shimadzu UV-2450 model and $BaSO_4$ used as the reference. SEM analysis was performed on a JEOL instrument with beam energy of 4 kV by placing the calcined MCM-41 and CNTs on conductive carbon tape. The TEM images of mesoporous MCM-41 and CNTs were obtained using a JEOL 3010 electron microscope operated at 300 kV. Samples for TEM were prepared by placing droplets of a suspension of the sample in acetone on a polymer micro grid supported on a Cu grid. Raman spectra were recorded with a Micro-Raman system RM 1000 Renishaw using a laser excitation line at 532 nm (Nd-YAG), 0.5 to 1 mW, with 1 μm focus spot in order to avoid the photodecomposition of the samples.

3. Results and discussion

3.1. Characterizations of metal-containing mesoporous MCM-41 molecular sieves

3.1.1. Elemental analysis

Elemental analyses of hydrothermally synthesized mesoporous Cr-MCM-41 molecular sieves were analyzed by ICP-AES. Table 1 represents the ICP analysis of catalysts Si/Cr of calcined samples. Under the synthesis conditions used, the Si/Cr ratio derived by the elemental analysis was nearly close to the gel composition as noticed in the mesoporous material. These results indicate that, almost all metal particles employed during synthesis were incorporated in the mesoporous materials.

3.1.2. Low-angle XRD analysis

Low-angle XRD technique was used to identify the pore structure of the Cr-MCM-41 materials. The XRD patterns of calcined incorporated materials are shown in Fig. 1. The calcined MCM-41 material show a strong peak in the 2θ range of 1.8–2.8° due to (1 0 0) diffraction lines and weak peaks in the 2θ range of 3.8–4.8° and 6.2–6.7° due to higher order such as (1 1 0), (2 0 0) and (2 1 0) diffractions indicating the formation of well-ordered hexagonal symmetry of MCM-41 mesoporous materials [9]. The appearance of same diffractogram after calcinations step suggests that MCM-41 has good thermal stability which was in agreement with Chenite et al. [19]. The d-spacing value decreased with increase in Cr concentration over the MCM-41 framework and the values are given in Table 1. The 2θ values found slightly shifted towards the higher region with increase in the Cr concentration which may be due to the shrinkage of the hexagonal pores. The intensity of the XRD peaks for Cr-MCM-41 decreases with increase in the Cr concentration, however the existence of same diffraction pattern even at higher loading (Si/Cr = 50) implies that the addition of chromium did not change the nature of MCM-41.

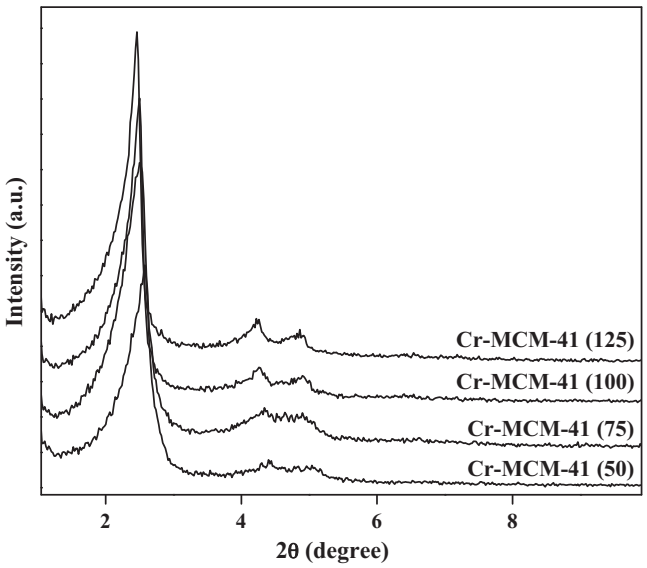

Fig. 1. XRD patterns of mesoporous Cr-MCM-41.

3.1.3. Nitrogen sorption isotherms

Table 1 show that BET surface area, pore size and pore volume of Cr-MCM-41 materials. The surface area, pore diameter and pore volume increased with the decrease in the Cr concentration over the MCM-41 molecular sieves. This might be due to shrinkage of bond and also some of the pores are blocked by the addition of metal particles. Fig. 2 shows the N_2 sorption isotherms of the materials with a sharp inflection at relative pressures (P/P_0) in the range of 0.21–0.33. This corresponds to the capillary condensation of N_2 in the mesopores with completely reversible isotherms characteristic of ordered mesoporous materials. All types of the isotherms were similar in shape and correspond to type IV curves indicating that the order of hexagonal arrays of mesopores in MCM-41 is not much affected on increasing the metal ratios. However, the position of the capillary condensation step shifted to some extent towards the lower partial pressure. The sharpness of the inflection reflects the uniformity of the pore sizes which is evident from Fig. 3.

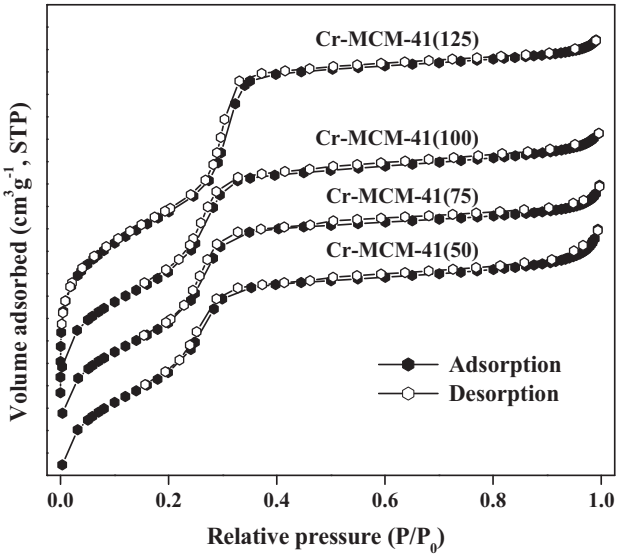

Fig. 2. Nitrogen sorption isotherms of mesoporous Cr-MCM-41.

Table 1
Textural properties of the mesoporous Cr-MCM-41.

Catalyst (Si/Cr ratio)[a]	(Si/Cr ratio)[b]	d-spacing (nm)[c]	Surface area (m^2/g)[d]	Pore size (nm)[d]	Pore volume (cc/g)[d]
Cr-MCM-41 (125)	127	3.715	897	2.912	0.756
Cr-MCM-41 (100)	102	3.698	855	2.875	0.714
Cr-MCM-41 (75)	79	3.676	840	2.752	0.698
Cr-MCM-41 (50)	54	3.643	822	2.704	0.687

[a] The values are calculated from the gel.
[b] The values obtained from ICP-AES analysis.
[c] The values obtained from XRD analysis.
[d] The values obtained from N_2 sorption studies.

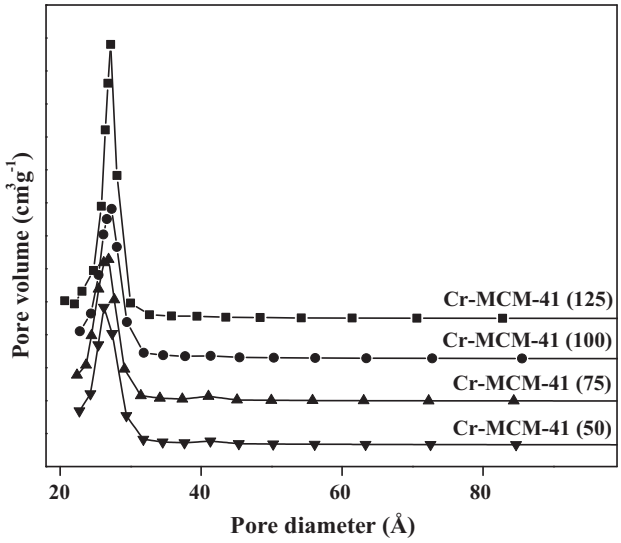

Fig. 3. Pore size distributions of mesoporous Cr-MCM-41.

3.1.4. Thermogravimetric analysis

Thermogravimetric analysis of the catalysts shows three distinct weight losses that depend on the framework composition as shown in Fig. 4. The first weight loss was observed between 50 and 150 °C is due to desorption of physisorbed water. The second stage of weight loss was between 150 and 350 °C, which corresponds to the decomposition of the surfactant species. Finally, the weight loss from 350 to 550 °C is assigned to the condensation of adjacent silanol (Si—OH) groups to form a siloxane bond [20,21]. After that there was no weight loss observed from thermogram; this suggests that MCM-41 mesoporous materials have high thermal stability.

3.1.5. DRS-UV measurements

In order to study the co-ordination environment of Cr in calcined Cr-MCM-41, DRS-UV was recorded and the results are shown in Fig. 5. Mesoporous Cr-MCM-41 catalysts were initially green in color and changed to yellow upon calcination. The former is due to the presence of trivalent chromium ions and latter is due to the presence of hexavalent chromium ions (viz., chromate and/or polychromate ions). Typical absorption bands with λ_{max} around 445 and 370 nm are corresponding to polychromate and chromate species, respectively. In addition, the band at 270 nm is due to trivalent chromium in octahedral co-ordination [22]. However, from the DRS-UV Visible studies, it can be concluded that the Cr in MCM-41 occupy different environment. The intensity of absorbance band for Cr-MCM-41 increases with increase in the Cr concentration which is clearly observed in Fig. 5.

3.1.6. TEM analysis

The structural morphology of Cr-MCM-41 at various ratios (Si/Cr ratios = 50, 75, 100 and 125), 0.2 wt.% Fe/Cr-MCM-41 (100) and 0.2 wt.% Pd/Cr-MCM-41 (100) were investigated by the TEM technique. The TEM images of these catalysts are presented in Fig. 6; the images indicate that the synthesized materials exhibited a well-ordered hexagonal array of regular pores commonly known for MCM-41 material [23]. The appearance of honeycomb structure in these materials indicates that the ordering of the hexagonal arrays is not much affected while increasing the metal content. The absence of any metal particles or cluster indicates that the added metal may be incorporated within the MCM-41 framework. Based on Fig. 10(a), the impregnated metal particle size was calculated and it is in the range of 4–5 nm. Similarly for Fig. 10(b) the size was in the range of 6–7 nm.

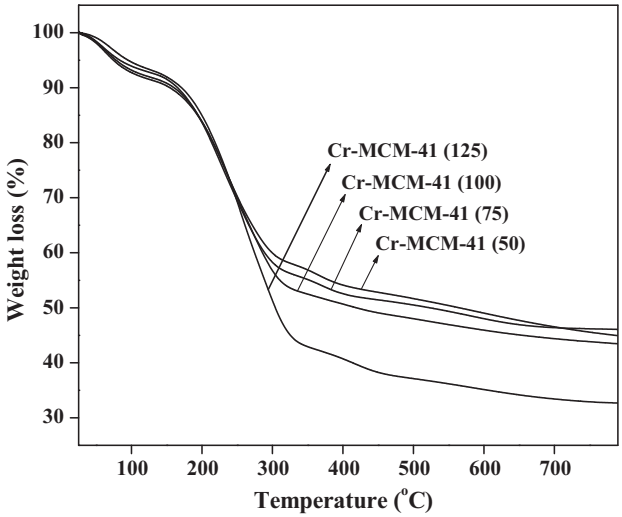

Fig. 4. TGA curves of as-synthesized mesoporous Cr-MCM-41.

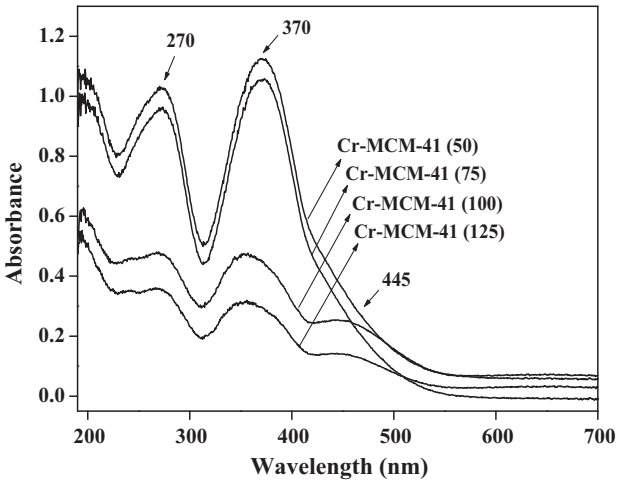

Fig. 5. DR-UV Visible spectra of mesoporous Cr-MCM-41.

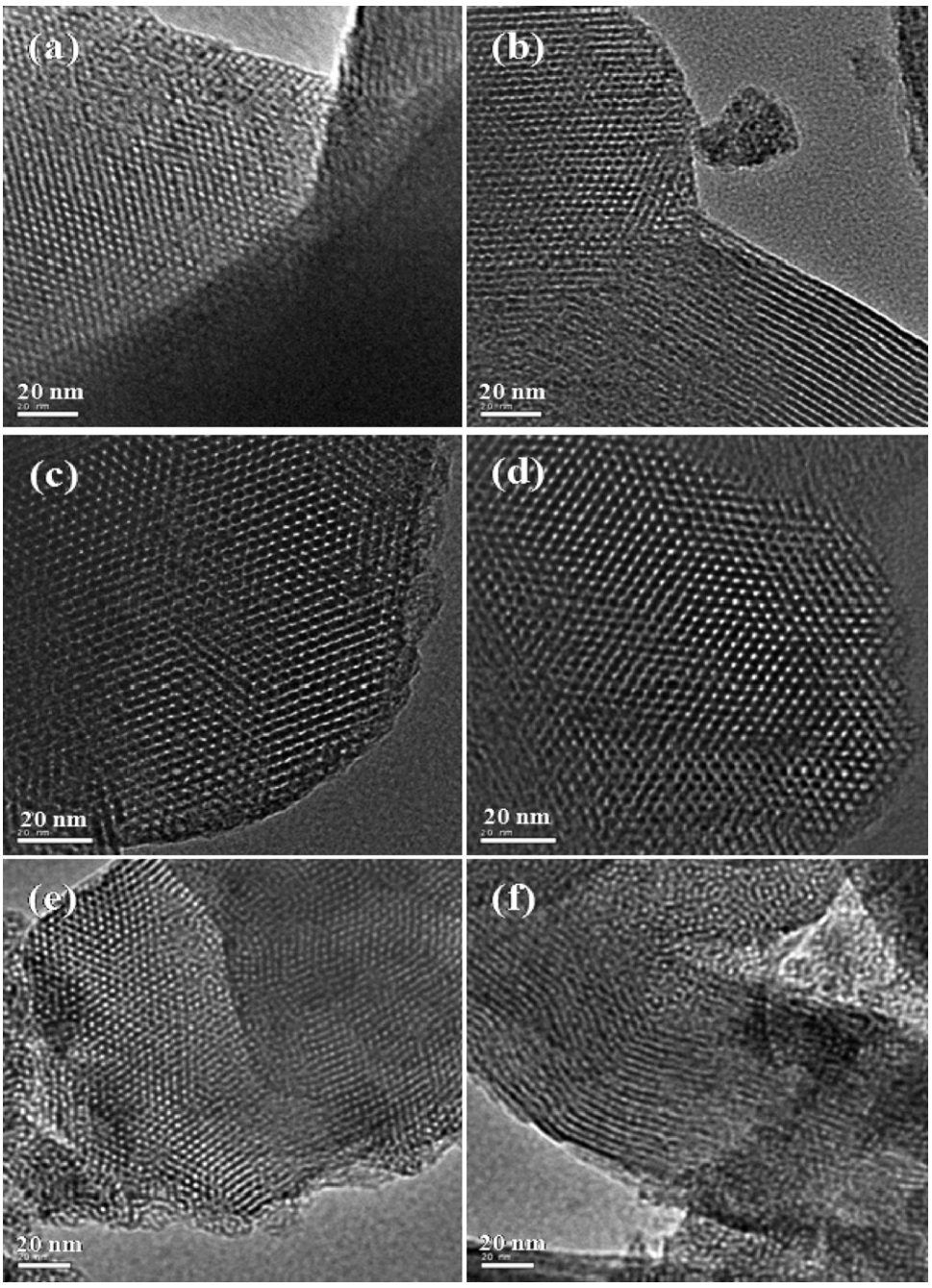

Fig. 6. TEM images of (a) Cr-MCM-41 (50), (b) Cr-MCM-41 (75), (c) Cr-MCM-41 (100), (d) Cr-MCM-41 (125), (e) 0.2 wt.% Fe/Cr-MCM-41 (100) and (f) 0.2 wt.% Pd/Cr-MCM-41 (100).

3.2. Formation of MWCNTs with respect to activity of the mesoporous molecular sieves

In order to study the effect of various catalysts on CNT formation, the synthesized catalysts were tested at 800 °C and the specific activity of the catalysts was calculated and they are in the order 1.13 (Cr-MCM-41 (100)) > 1.0 (Cr-MCM-41 (75)) > 0.99 (Cr-MCM-41 (125)) > 0.87 (Cr-MCM-41 (50)). Further, the effect of various temperature (700, 750, 800, 850 and 900 °C) on the formation of MWCNTs was carried over Cr-MCM-41 (100). The deposition of MWCNTs with respective reaction temperature are shown in the following order 800 °C > 850 °C > 750 °C > 900 °C > 700 °C and the optimized temperature for better formation of MWCNTs is marked in bold letters (Table 2). The amount of metals (Cr)

Table 2
Influence of temperature and C_2H_2 flow rate for carbon deposition at the reaction time of 30 min.

Catalyst (Si/Cr ratio)	Reaction temperature (°C)	Flow rate of acetylene (mL/min)	Carbon deposition (%)
	700	100	76
	750	100	100
	800	100	113
	850	100	107
Cr-MCM-41 (100)	900	100	95
	800	25	50
	800	50	65
	800	75	86
	800	125	111

Table 3
Influence of various metal-containing mesoporous catalysts for carbon deposition at the reaction time of 30 min.

Catalyst (Si/Cr ratio)	Reaction temperature (°C)/flow rate of acetylene (mL/min)	Carbon deposition (%)
Cr-MCM-41 (125)	800/100	99
Cr-MCM-41 (100)	800/100	113
Cr-MCM-41 (75)	800/100	100
Cr-MCM-41 (50)	800/100	87
Fe/Cr-MCM-41	800/100	145
Co/Cr-MCM-41	800/100	134
Ni/Cr-MCM-41	800/100	140
Mn/Cr-MCM-41	800/100	138
Ru/Cr-MCM-41	800/100	137
Pd/Cr-MCM-41	800/100	144
Ti/Cr-MCM-41	800/100	131

present in the MCM-41 decides the activity of the catalysts. The lower activity at higher loading of Cr might be due to irregular dispersion of active species and results in the formation of bulk and clustered metal particles. This reduces the existence of active sites and surface area, thereby hinders the growth of MWCNTs. The influence of temperature on MWCNTs growth was also studied and results show that the carbon deposition increases with increase in temperature and found to be optimum at 800 °C. Further increase leads to decrease in the yield. The decrease in MWCNTs yield at lower and higher temperature is due to the formation of carbonaceous impurities and self-pyrolysis at elevated temperature respectively (Fig. 9). In order to improve the growth of MWCNTs on Cr-MCM-41 (100), loading of second metal (Fe, Co, Mn, Ni, Ti, Ru and Pd) with 0.2 wt.% was conducted at 800 °C. The catalytic activity for the deposition of carbon materials was found to be increasing in the case of Fe loaded catalyst. The carbon deposition yield (%) decreasing trend was observed in the following order: Fe/Cr-MCM-41(100) ≈ Pd/Cr-MCM-41(100) > Ni/Cr-MCM-41(100) > Mn/Cr-MCM-41(100) > Ru/Cr-MCM-41(100) > Co/Cr-MCM-41 (100) > Ti/Cr-MCM-41(100) > Cr-MCM-41(100). When compared with other bimetal loaded MCM-41, Fe/Cr-MCM-41 and Pd/Cr-MCM-41 showed the better MWCNTs growth at 800 °C which is marked in bold letters (Table 3). This might be due to the evenly dispersed metal particles over the support and the existence of more number of active sites. Among the catalysts Fe/Cr-MCM-41 and Pd/Cr-MCM-41 showed higher specific activity then others. It was attributed to very fine dispersion metal particles which was also evident from the TEM images (Fig. 10(a) and (b)). Hence, based on the specific activity the particle size distribution in Fe/Cr-MCM-41 was in the range of 4–6 nm and in Pd/Cr-MCM-41 in the ranges of 6–7 nm. The growth percentage of MWCNTs is also dependent on the flow rate of acetylene. Large quantity and well graphitized MWCNTs were grown at the flow rate of acetylene is 100 mL/min. The growth percentages of MWCNTs were decreased at the flow rate below 100 mL/min due to the deficiency of acetylene at the time of NTs growth. The amorphous carbon leads to the formation of MWCNTs when the flow rate of acetylene is high. Formation of CNT was evident with Cr-MCM-41, Fe/Cr-MCM-41 and Pd/Cr-MCM-41. The carbon deposition and yield of MWCNTs over Fe/Cr-MCM-41 and Pd/Cr-MCM-41 were higher than Cr-MCM-41. Hence Fe/Cr and Pd/Cr were active for the formation of CNTs and cumulative effect of bimetal catalysts was also evident from the study.

3.3. Characterization of MWCNTs

3.3.1. SEM analysis

The SEM images of as-synthesized MWCNTs with different Si/Cr ratio (Si/Cr ratio = 50, 75, 100 and 125) at constant reaction temperature (800 °C) and constant Si/Cr ratio (100) with various reaction temperatures (700–900 °C) are shown in Fig. 7. The MWCNTs appeared as filaments are seen clearly and this indicates the formation of CNTs over the mesoporous materials. The SEM images of as-synthesized CNT grown over Co, Fe, Mn, Ni, Ti, Ru and Pd loaded Cr-MCM-41 at 800 °C were shown in Fig. 8. In addition to chromium, the catalytically active ingredients such as Co, Fe, Mn, Ni, Ti, Ru, and Pd metal particles that are present over the surface induces the formation of MWCNTs. The CNTs are distributed uniformly throughout the matrix, as they grow where the active ingredients are present. Large number of carbon filaments was produced over Fe/Cr-MCM-41 and Pd/Cr-MCM-41 mesoporous catalytic templates which were observed from SEM images. The formed MWCNTs were purified in order to remove carbonaceous impurities as well as remaining mesoporous materials and these were analyzed by SEM. The absence of catalytic templates (Fe/Cr-MCM-41 and Pd/Cr-MCM-41) in the purified MWCNTs is observed from SEM images as shown in Fig. 8(h) and (i).

3.3.2. TEM analysis

The TEM images of as-synthesized MWCNTs grown over Fe/Cr-MCM-41 at different temperatures are shown in Fig. 9. The carbonaceous matters were increased in MWCNTs at lower and higher temperature is due to the formation of carbonaceous impurities and self-pyrolysis respectively. This was clearly observed in Fig. 9(a) and (c). The synthesized MWCNTs contain impurities such as metal catalysts, amorphous carbons and microcrystalline carbons, which normally make more complex for the detection of MWCNTs by TEM. The TEM images of purified MWCNTs grown on Fe/Cr-MCM-41 and Pd/Cr-MCM-41 are shown in Fig. 10. The clear visible MWCNTs were observed after purification by acid treatment and air oxidation which indicates majority of the impurities were eliminated. The inner and outer diameter of the synthesized MWCNTs was calculated from TEM images, which is in the range of 4–5 nm and 12–13 nm for the case of Fe/Cr-MCM-41, 6–7 nm and 16–17 nm for Pd/Cr-MCM-41. From TEM studies, it can be observed that a very less quantity of amorphous carbon was deposited on the surface of MWCNTs because it was prepared from acetylene using active Fe/Cr-MCM-41 and Pd/Cr-MCM-41 catalytic templates. The results revealed that a high quality MWCNTs were obtained. In general the formation of CNTs explained by tip growth and base growth mechanism. Tip growth mode involves the weak metal–support interaction where as in base growth mode the interaction is strong [24]. The obtained TEM images show that the metal particles are present over the tip of the MWCNT as represented in Fig. 10(a) and the magnified TEM images clearly indicates that the metal particles are present in the tip of MWCNTs (Fig. 11). Hence, it can be concluded that the mechanism follows the tip growth but not the base growth. The present study confirms the quality production of MWCNTs through decomposition of acetylene over the Fe/Cr-MCM-41 and Pd/Cr-MCM-41 by CVD method. The MWCNTs formed over Fe/Cr-MCM-41 possessed higher quality than that over Pd/Cr-MCM-41. It was clearly evident from TEM images and Raman spectrum.

3.3.3. Thermogravimetric analysis

The as-synthesized MWCNT samples, synthesized over Fe/Cr-MCM-41 (100) at different temperatures (700, 800 and 900 °C) were subjected to thermal studies and their TGA curves are shown in Fig. 12. The as-grown samples were heated from 30 to 900 °C in N_2 atmosphere (heating rate = 20 °C/min). The MWCNTs obtained at 700 and 900 °C, showed a trace amount of weight loss occurred above 600 and 700 °C, respectively. The carbonaceous impurities (amorphous carbon, microcrystalline carbon and also SWCNTs) deposited over the MWCNTs were decomposed (eliminated) at lower temperature. The MWCNTs obtained at 700 and 900 °C

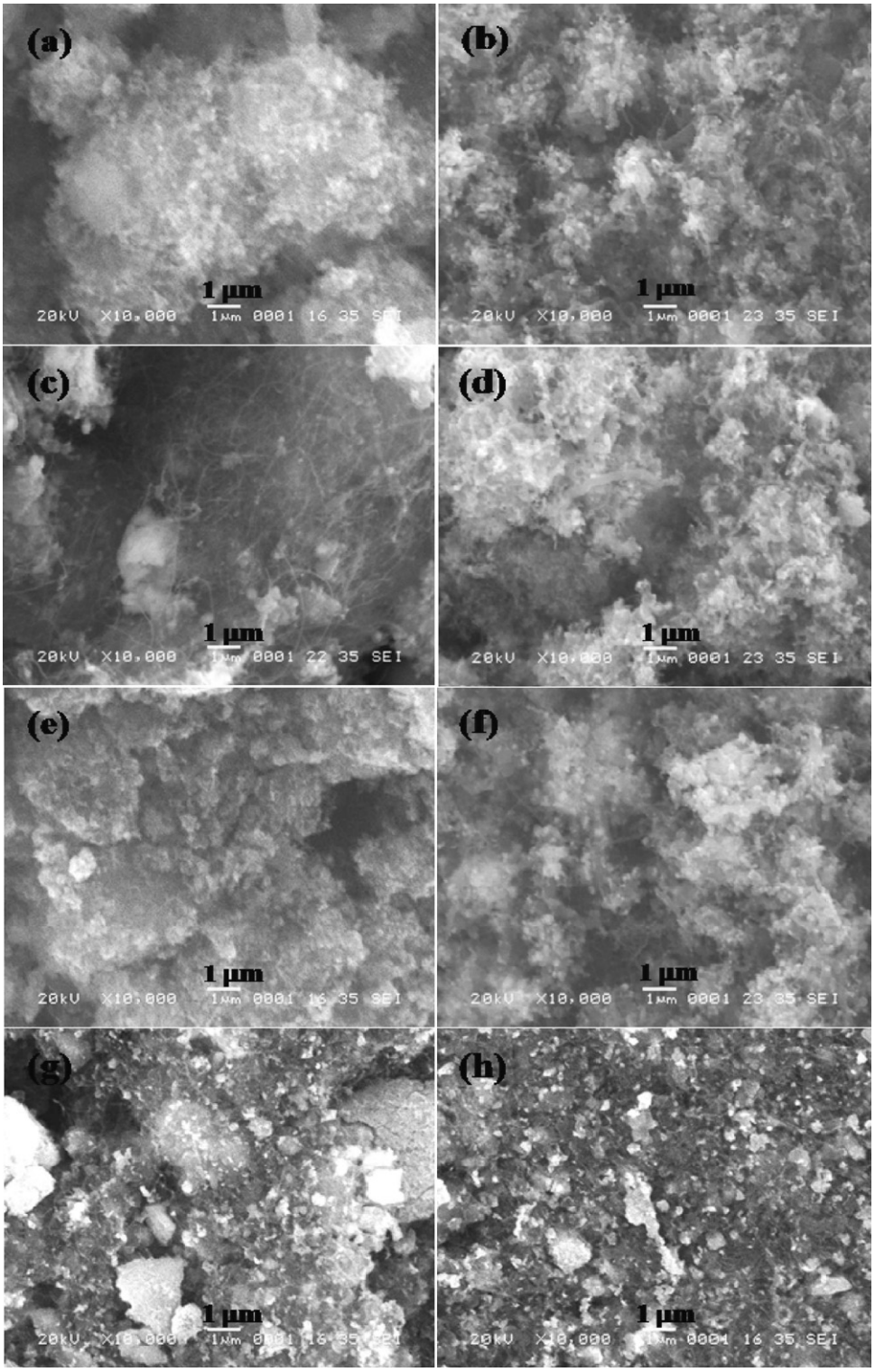

Fig. 7. SEM images of as-synthesized MWCNTs at 800 °C over: (a) Cr-MCM-41 (50), (b) Cr-MCM-41 (75), (c) Cr-MCM-41 (100) and (d) Cr-MCM-41 (125); SEM images of as-synthesized MWCNTs over Cr-MCM-41 (100) at: (e) 700 °C, (f) 750 °C, (g) 850 °C and (h) 900 °C.

contained higher content of carbonaceous impurities than that obtained at 800 °C. It was due to self-pyrolysis of MWCNTs produced at elevated temperature, the TEM image also confirmed it. The combustion of amorphous carbon and SWCNTs take place at lower than the decomposition temperature of MWCNTs [25]. There was no weight loss up to 800 °C, and beyond that it was very low. Therefore, MWCNTs grown over Fe/Cr-MCM-41 at 800 °C contained very low percentage (negligible amount) of carbonaceous impurities. The quality of the order of temperature for the MWCNTs was 800 °C > 900 °C > 700 °C. Hence, the thermal study confirmed that the MWCNTs obtained over Fe/Cr-MCM-41 at 800 °C were pure and thermally stable due to the constructions of well graphitized walls.

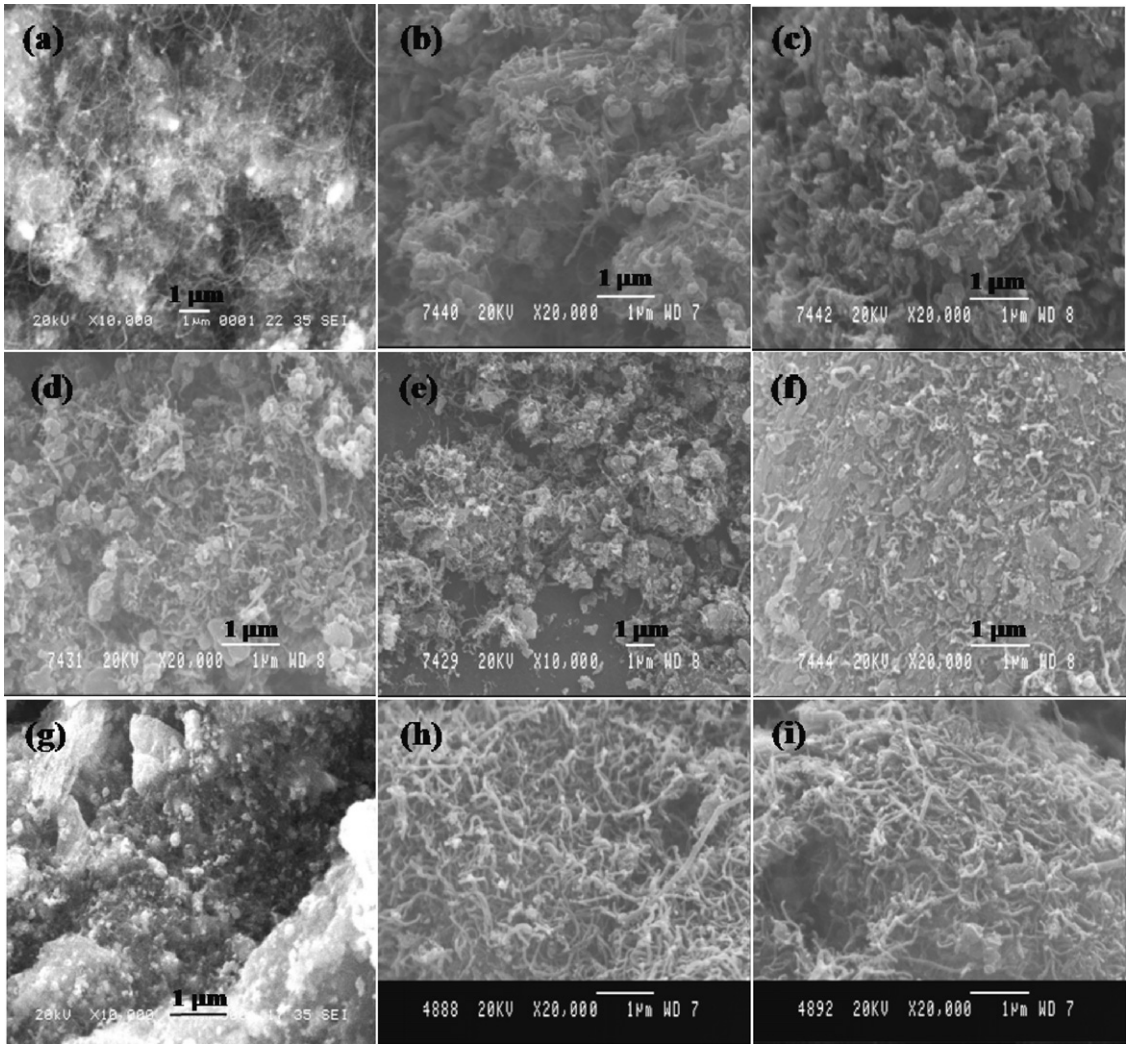

Fig. 8. SEM images of as-synthesized MWCNTs at 800 °C over (a) Fe/Cr-MCM-41, (b) Pd/Cr-MCM-41, (c) Ni/Cr-MCM-41, (d) Mn/Cr-MCM-41, (e) Ru/Cr-MCM-41, (f) Co/Cr-MCM-41 and (g) Ti/Cr-MCM-41; SEM images of purified MWCNTs formed over (h) Fe/Cr-MCM-41 and (i) Pd/Cr-MCM-41.

3.3.4. XRD analysis

High-angle XRD pattern of MWCNT is shown in Fig. 13. The pattern shows a strong peak at $2\theta = 26.30^{\circ}$ and weak peak at $2\theta = 42.10^{\circ}$, which are assigned to (0 0 2) and (1 0 0) diffraction patterns of typical graphite, respectively. The results confirmed that the MWCNTs are well graphitized [26]. Hence, there is very less amount of impurity present in the purified MWCNTs, which is observed in XRD patterns and was confirmed by the TEM images.

3.3.5. Raman spectroscopy

Raman spectroscopy is one of the most powerful tools for characterization of CNTs. Fig. 14 shows the Raman spectra of purified MWCNTs synthesized using Fe/Cr-MCM-41 and Pd/Cr-MCM-41. The two major peaks around 1600 and 1350 cm^{-1} correspond to graphite band (G-band) and disorder band (D-band) respectively. The G-band observed around 1600 cm^{-1} is assigned to the Raman-allowed phonon E_{2g} (stretching) mode of graphite. The strongest

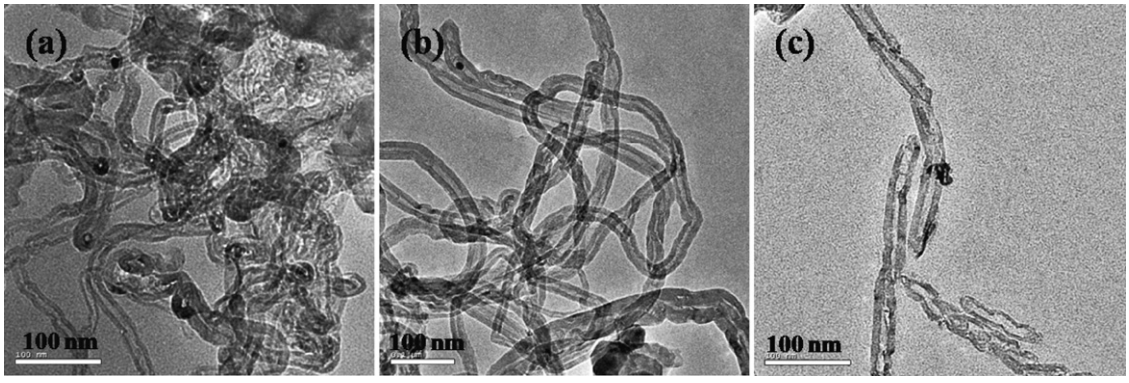

Fig. 9. TEM images of as-synthesized MWCNTs over Fe/Cr-MCM-41 at (a) 700 °C (b) 800 °C and (c) 900 °C.

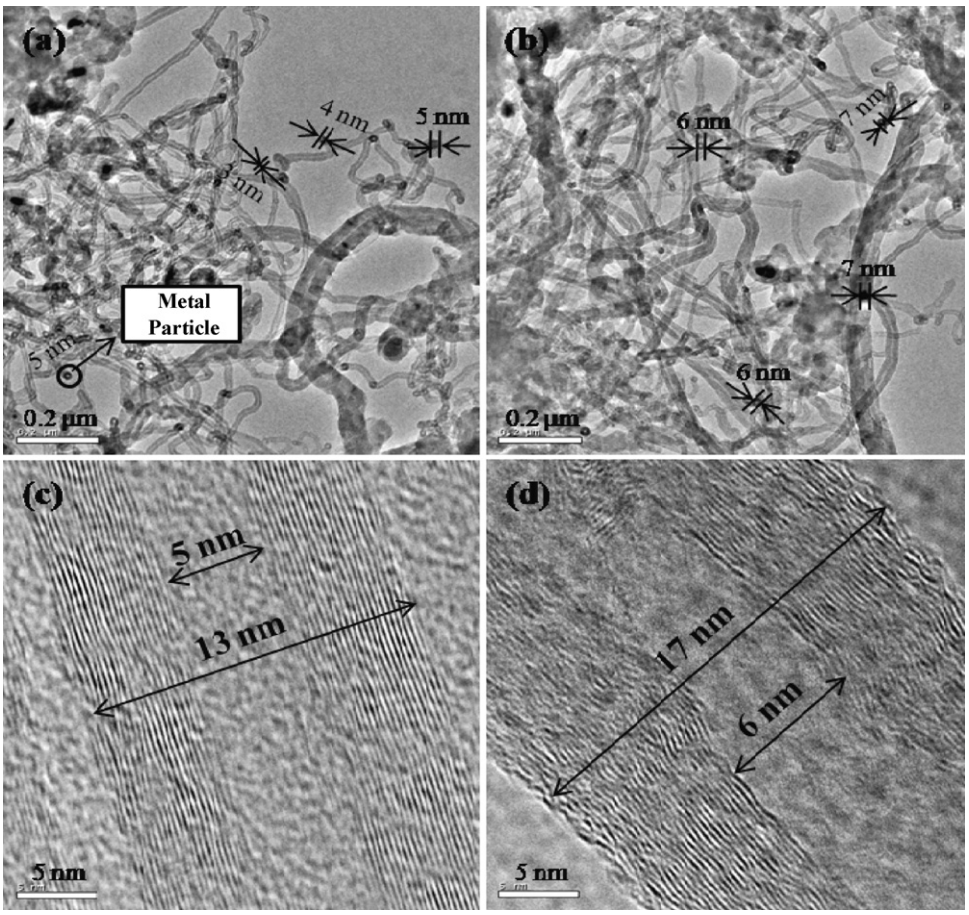

Fig. 10. TEM images of purified MWCNTs with different magnification formed over (a) and (c) Fe/Cr-MCM-41, (b) and (d) Pd/Cr-MCM-41.

peak of G-band in the spectrum indicates the formation of good arrangement of hexagonal lattice of graphite. The band around 1350 cm^{-1} corresponds to the D-band; the weak D-band confirms the high purity and assigned to the A_{1g} phonon. The very high I_G/I_D values obtained in the Raman spectrum clearly indicated the synthesized MWCNTs have high purity and well graphitized [27,28]. The absence of radial breathing mode (RBM) below 500 cm^{-1} confirms the absence of SWCNTs in the synthesized carbon materials. The present investigation suggests that a high quality of MWCNTs without SWCNTs, metallic clusters and other carbonaceous impurities can be obtained from Fe/Cr-MCM-41 and Pd/Cr-MCM-41 molecular sieves by CVD.

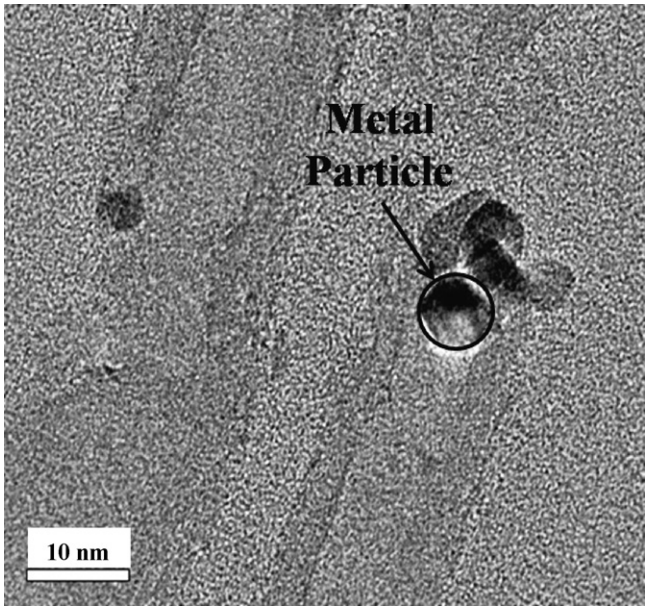

Fig. 11. HR-TEM image of MWCNT with metal particles end of the top.

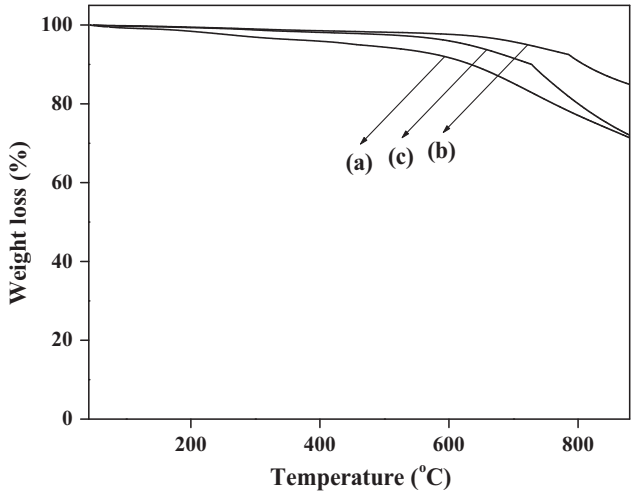

Fig. 12. TGA curves (under N_2 atmosphere) of as-synthesized MWCNTs obtained over Fe/Cr-MCM-41 at (a) 700 °C (b) 800 °C and (c) 900 °C.

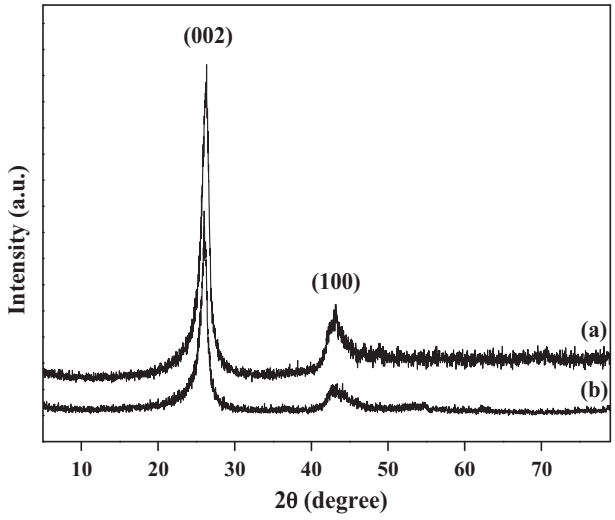

Fig. 13. XRD patterns of purified MWCNTs formed over (a) Fe/Cr-MCM-41 and (b) Pd/Cr-MCM-41.

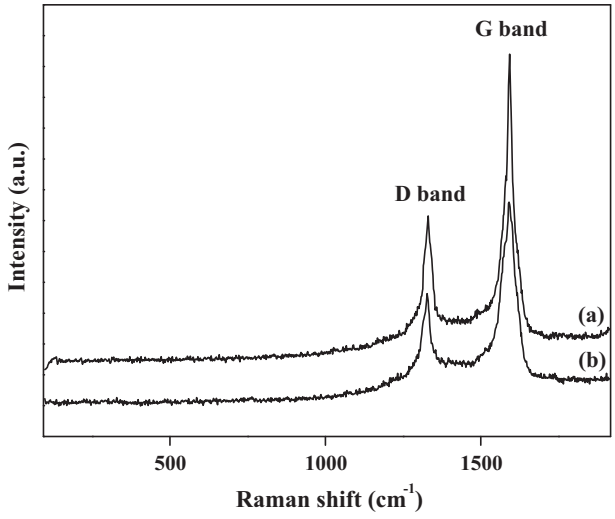

Fig. 14. Raman spectra of purified MWCNTs formed over (a) Fe/Cr-MCM-41 and (b) Pd/Cr-MCM-41.

4. Conclusion

Structural stability, thermal stability, porosity and morphology of Cr-MCM-41 and M/Cr-MCM-41 (where *M* = Fe, Co, Mn, Ni, Ti, Ru and Pd) materials were confirmed by various physico-chemical techniques. MWCNTs were catalytically synthesized by the decomposition of acetylene using Cr-MCM-41 and M/Cr-MCM-41 catalyst at 800 °C. The combination of Fe or Pd with Cr was found to be more active to produce MWCNTs with high purity and great magnitude when compared with that produced by other mono and bimetallic catalysts. The absence of the catalytic template in MWCNTs was confirmed by SEM and TEM images of purified MWCNTs. The formation of MWCNTs with uniform inner diameter in the range of 4–5 nm and outer diameter in the range of 12–13 nm was observed in the case of Fe/Cr-MCM-41. The Pd/Cr-MCM-41 catalytic template was produced MWCNTs in the diameter range of 6–7 nm and 16–17 nm inner and outer, respectively. The high quality of MWCNTs arrays without major contamination is observed from HR-TEM. High qualities of MWCNTs without SWCNTs and other carbonaceous impurities were confirmed by Raman studies. The good thermal stability and high productivity revealed from those studies suggested that the Fe/Cr-MCM-41 and Pd/Cr-MCM-41 mesoporous molecular sieves could be promising supports for catalytically synthesizing MWCNTs by CVD.

Acknowledgments

The authors would like to thank the Department of Science and Technology (SR/S5/NM-35/2005) under Nanoscience and Technology Initiative and Council of Scientific and Industrial Research, New Delhi, India, for providing financial support. The authors would like to thank the Department of Chemistry, Anna University, Chennai, India, for providing instrumentation facilities to carry out characterization.

References

[1] S. Iijima, Nature 354 (1991) 56–58.
[2] S. Iijima, T. Ichihashi, Nature 363 (1993) 603–605.
[3] Y. Saito, S. Uemura, Carbon 38 (2000) 169–182.
[4] E. Frackowiak, F. Beguin, Carbon 40 (2002) 1775–1787.
[5] L.A. Gevorgian, K.A. Ispirian, R.K. Ispirian, Nucl. Instrum. Meth. Phys. Res. Sect. B 145 (1998) 155–159.
[6] R.B. Little, J. Cluster Sci. 14 (2003) 135–185.
[7] J. Zhu, M. Yudasaka, S. Iijima, Chem. Phys. Lett. 380 (2003) 496–502.
[8] C.T. Kresge, M.E. Leonowicz, W.J. Roth, J.C. Vartuli, J.S. Beck, Nature 359 (1992) 710–712.
[9] J.S. Beck, J.C. Vartuli, W.J. Roth, M.E. Leonowicz, C.T. Kresge, K.D. Schmitt, C.T.W. Chu, D.H. Olson, E.W. Sheppard, S.B. McCullen, J.B. Higgins, J.L. Schlenker, J. Am. Chem. Soc. 114 (1992) 10834–10843.
[10] A. Corma, Chem. Rev. 97 (1997) 2373–2419.
[11] Y. Chen, D. Ciuparu, S. Lim, G.L. Haller, L.D. Pfefferle, Carbon 44 (2006) 67–78.
[12] T. Somanathan, A. Pandurangan, Ind. Eng. Chem. Res. 45 (2006) 8926–8931.
[13] Y. Li, W. Kim, Y. Zhang, M. Rolandi, D. Wang, H. Dai, J. Phys. Chem. B 105 (2001) 11424–11431.
[14] M. Anna, G.N. Albert, I.K. Esko, J. Phys.: Condens. Matter 15 (2003) S3011–S3035.
[15] C. Oncel, Y. Yurum, Fuller. Nanotub. Car. N 14 (2006) 17–37.
[16] B. Zheng, Y. Li, J. Liu, Appl. Phys. A 74 (2002) 345–348.
[17] M. Urban, D. Mehn, Z. Konya, I. Kiricsi, Chem. Phys. Lett. 359 (2002) 95–100.
[18] T. Suzuki, S. Inoue, Y. Ando, Diamond Relat. Mater. 17 (2008) 1596–1599.
[19] A. Chenite, Y. Lepage, A. Sayari, Chem. Mater. 7 (1995) 1015–1019.
[20] M.L. Occelli, S. Biz, A. Auroux, G.J. Ray, Microporous Mesoporous Mater. 26 (1998) 193–213.
[21] S. Vetrivel, A. Pandurangan, J. Mol. Catal A: Chem. 227 (2005) 269–278.
[22] C. Mahendiran, P. Sangeetha, P. Vijayan, S.J. Sardhar Basha, K. Shanthi, J. Mol. Catal. A: Chem. 275 (2007) 84–90.
[23] S. Lim, D. Ciuparu, Y. Yang, G. Du, L.D. Pfefferle, G.L. Haller, Microporous Mesoporous Mater. 101 (2007) 200–206.
[24] R.T.K. Baker, Carbon 27 (1989) 315–323.
[25] S. Scaccia, M. Carewska, P.P. Prosini, Thermochim. Acta 435 (2005) 209–212.
[26] J.C. Juan, Y. Jiang, X. Meng, W. Cao, M.A. Yarmo, J.C. Zhang, Mater. Res. Bull. 42 (2007) 1278–1285.
[27] R. Zhang, X. Wang, Chem. Mater. 19 (2007) 976–978.
[28] S. Shanmugam, A. Gedanken, J. Phys. Chem. B 110 (2006) 2037–2044.